Available online at www.sciencedirect.com

SCIENCE DIRECT®

Vision Research 44 (2004) 839–848

Vision Research

www.elsevier.com/locate/visres

Reducing noise in suspected glaucomatous visual fields by using a new spatial filter ☆

Stuart K. Gardiner [a], David P. Crabb [a,*], Fred W. Fitzke [b], Roger A. Hitchings [c]

[a] *Faculty of Science, Nottingham Trent University, Clifton Campus, Nottingham NG11 8NS, UK*
[b] *Institute of Ophthalmology, London EC1V 9EL, UK*
[c] *Glaucoma Unit, Moorfields Eye Hospital, London EC1V 2PD, UK*

Received 11 December 2002; received in revised form 8 May 2003

Abstract

Visual field testing with automated perimetry is hampered by the amount of noise present in the readings. Here, we derive a physiologically accurate spatial filter to be applied to the data after patient examination. The filter was tested by a Virtual Eye computer simulation. By simulating series of stable fields it was shown that specificity of determining visual field changes was improved; while simulating progressing fields (based on a map of the optic nerve head) it was shown that sensitivity was also improved. The filter appears to reduce the noise in glaucomatous visual field data and may be clinically useful.

Keywords: Visual field; Perimetry; Glaucoma; Optic nerve head; Statistics

1. Introduction

Reliable detection of glaucomatous visual field defects, and follow-up of current defects to determine whether they are spreading or deepening, is crucial for correct management of patients. Yet this is extremely difficult given the inaccuracy of threshold perimetry (in terms of the high inter-test and intra-test variability) and the various components of variability (or noise) associated with the perimetric process (Chauhan & House, 1991; Flammer, Drance, & Zulauf, 1984; Spenceley & Henson, 1996; Spry & Johnson, 2002; Wild, Searle, Dengler-Harles, & O'Neill, 1991). Therefore, it is sought to find ways of reducing the noise present in the readings. Reducing this noise is particularly relevant when detecting visual field progression (Spry & Johnson, 2002): true change in a glaucomatous visual field has to be larger than the noise before it becomes statistically distinguishable (Chauhan & Johnson, 1999; Heijl, Lindgren, & Olsson, 1989). Improved methods of data acquisition (Bengtsson, Olsson, Heijl, & Rootzén, 1997) have tended to focus on reducing the time of perimetric examination rather than making the measurement more accurate (Artes, Iwase, Ohno, Kitazawa, & Chauhan, 2002; Wild, Pacey, O'Neill, & Cunliffe, 1999). Carrying out more readings during the testing procedure is also clearly undesirable. Far better would be to process the data in such a way that the noise would be reduced, without any additional testing time. One way of doing this relies on exploiting the relationships between the actual sensitivities of different points; in essence, if one point has a reduced sensitivity, then its neighbours are more likely to also have reduced sensitivities. This principle points towards spatial filtering of the data as a possible solution.

Spatial filtering is a widely used image processing technique used to improve the quality of digital information. Spatial filtering applied to perimetric threshold sensitivity values using a Gaussian filter (fully described elsewhere by Crabb, Edgar, Fitzke, McNaught, & Wynn, 1995; Fitzke, Crabb, McNaught, Edgar, & Hitchings, 1995, and illustrated in Fig. 1) has been show to reduce test–retest variability and reduce measurement noise (Crabb, Fitzke, McNaught, Edgar, & Hitchings,

☆ This work has not been published elsewhere and is not under review with another journal. If published in *Vision Research* it will not be reprinted elsewhere in any language in the same form without the consent of the publisher, who holds the copyright.

* Corresponding author. Tel.: +44-115-848-3275; fax: +44-115-848-6690.

E-mail address: david.crabb@ntu.ac.uk (D.P. Crabb).

0042-6989/$ - see front matter © 2004 Elsevier Ltd. All rights reserved.
doi:10.1016/S0042-6989(03)00474-7

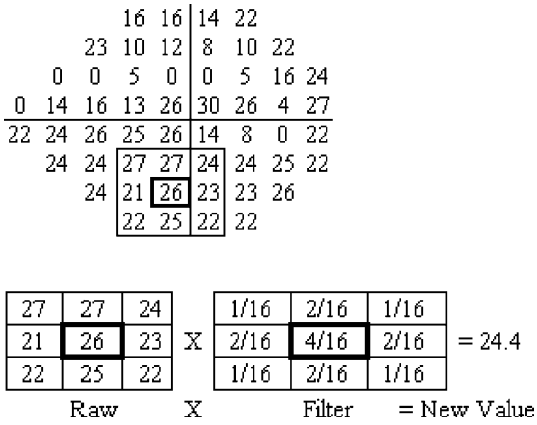

Fig. 1. How the new sensitivity is calculated by the Gaussian filter. In this method, the raw sensitivity value is replaced by one derived from a linear combination of the sensitivities at the nine points in a square centred on the point of interest. This is repeated for each point in the field in turn, each time looking at the points in a square surrounding the point of interest.

1997). Moreover, benefits from post-test filtering of the data are accrued without any extra patient testing or alteration to the perimetric process.

However, there are problems with the basic Gaussian filter when applied to perimetric data. The visual field test locations, unlike say pixel values in digital images, are not physiologically linked in a 'grid-like' fashion as indicated by the matrix of values on the visual field chart and the Gaussian filter takes no account of the actual anatomical structure of the optic disc. For example, glaucomatous defects are generally limited to either the superior hemifield or the inferior hemifield; they rarely cross the horizontal meridian that passes through the fovea (Lachenmayr & Vivell, 1993). Yet the Gaussian filtered value at a point adjacent to this meridian is based in part on values from the opposite hemifield. There is general (albeit vague) agreement about the shape of the nerve fibre layer, and that the shapes of glaucomatous defects follow the nerves; the Gaussian filter ignores this information. It has been reported that applying the Gaussian filter to data may reduce the proportion of false positives (i.e. the number of healthy points flagged as being part of a defect), but it also reduces the detection of true positives, blurring out true defects (Spry, Johnson, Bates, Turpin, & Chauhan, 2002). This study aims to derive a filter taking into account the true structure of the retinal nerve fibre layer, that will reduce the noise without obscuring true defects.

2. Methods

The work is based on a visual fields database consisting of patients seen by the Moorfields Eye Hospital Glaucoma Service in London, UK. This means that the filter is based on, and designed for use in, a tertiary glaucoma referral service. It would be feasible to utilise the methods below to produce a filter for different situations, such as population screening events or general ophthalmic clinical settings; however the process would be hindered by the increased proportion of non-glaucomatous defects. It would be expected that the results would be extremely similar, although obviously that cannot be definitively assumed without testing. The database contains 98,821 visual fields, taken from 14,675 individual suspected glaucomatous patients. Fields were measured using the Humphrey Visual Field Analyser (Humphrey Instruments Inc., Dublin, California, USA). The data goes back as far as 1985; it consists of both 30-2 fields and more recently 24-2 fields (all standard white-on-white, full threshold tests), although only complete 24-2 fields (the non-edge points in 30-2 fields) were used. This database, consisting of around 5 million individual threshold values, provides an excellent resource giving a comprehensive and representative cross-section of all tests carried out at glaucoma clinics. The database was cleaned to remove duplicated visual fields; and each patient given a unique ID number. This way, the data was completely anonymised. Visual fields from right eyes were transposed, and their mirror images used instead as 'left' eyes.

2.1. Deriving the filter

When deriving the new filter, no patients were excluded. It was sought to use as representative a sample as possible of all the patients entering the clinic, on an "intention-to-treat" basis. A filter derived purely on data from glaucomatous patients may not be accurate for healthy eyes, and vice-versa; so all available data was used in the belief that this gives added weight to our results. This means that the results are truly representative of the average test carried out in a glaucoma clinic.

It is important to note that unreliable fields, or fields from patients presenting at the glaucoma clinic who turn out to have other pathologies (e.g. pituitary tumours, myelinated nerve fibres etc.), were not removed from the database prior to analysis. This is because we seek to represent the typical test carried out at a glaucoma clinic, and so these patients should not be ignored. The principle of "intention-to-treat" is well founded, and is very commonly used throughout the scientific and statistical literature. A further important distinction should be drawn between using every available test from each patient (making the results representative of the average visual field test carried out in a glaucoma clinic) and using one randomly selected field from each patient (which would make the results representative of the average patient seen by a glaucoma clinic). Since patients with true glaucoma would be expected to have

more fields in the database than patients with other pathologies, and since it is more important to deal with patients with glaucoma who make repeated visits to the clinic, the choice was made to use all the fields from each patient.

First, the covariances and correlations between sensitivities at each pair of points in the eye were found. For the covariance between sensitivities at points A and B,

$$\mathrm{Cov}(S_\mathrm{A}, S_\mathrm{B}) = E(S_\mathrm{A}S_\mathrm{B}) - E(S_\mathrm{A})E(S_\mathrm{B}) \tag{1}$$

where $E(S_\mathrm{A})$ is the expected (mean) value of the sensitivity at A, etc. Now, suppose we can accurately predict the sensitivity at point A by a linear combination of the sensitivities at all the other points

$$\widehat{S}_\mathrm{A} = k_1 S_1 + k_2 S_2 + k_3 S_3 + \cdots \tag{2}$$

for some constants $k_1, k_2, \ldots$; then from Eq. (1),

$$\mathrm{Cov}(S_\mathrm{A}, S_\mathrm{B}) = \sum_i k_i \mathrm{Cov}(S_i, S_\mathrm{B}) \tag{3}$$

We choose to perform regressions on the covariances in Eq. (3) rather than on the basic sensitivities in Eq. (2). This is because an apparent relationship between two points, X and Y say, may actually be the product of relationships between each of these points and some third point Z; looking at covariances takes account of this second-order of complexity. Before performing multiple regressions to find these coefficients k_i for each point A, a few constraints were placed on the regressions. Firstly, each k_i had to be non-negative. Secondly, the expected predicted value must equal the expected raw value for the filter to make sense; so

$$E(\widehat{S}_\mathrm{A}) = \sum_i k_i E(S_i) = E(S_\mathrm{A})$$

Finally, if the correlation between the sensitivities at point A and point i was low (less than 0.7), k_i was set to equal zero, as those points were considered to be unrelated (this was done mainly for computational reasons. In tests on small samples with fewer points it had no effect on the outcome; the regression still identified the same points as being good predictors with associated high values of k_i. In fact a small minority of the k_i were constrained to be zero because of this rule; far more were found to be zero after the regressions were carried out).

So, for each point A, regressions were performed on these series of equations (one equation for each point B) to produce constants k_i, and hence an algorithm for predicting the sensitivity at point A based on those at points elsewhere in the visual field.

The next stage is to produce the filtered value S_A^f for the sensitivity at point A; which should be a combination of the predicted sensitivity and the raw sensitivity at that point.

$$S_\mathrm{A}^\mathrm{f} = c\widehat{S}_\mathrm{A} + (1-c)S_\mathrm{A} \tag{4}$$

The value of c in Eq. (4) will vary according to the position in the eye; some points are more predictable than others, and these points should have a correspondingly high value of c, hence giving more weight to the predicted value. (Note that in the Gaussian filter, $c = 12/16$ for all points not adjacent to either the edge of the field or the blind spot, as shown in Fig. 1). Further, the more points that are used in the prediction (i.e. the greater the number of non-zero k_i), the more accurate this predicted value would be. Now, if the predictions were entirely accurate, the variance of the filtered value would be

$$\begin{aligned}\mathrm{Var}(S_\mathrm{A}^\mathrm{f}) &= \mathrm{Var}(c\widehat{S}_\mathrm{A} + (1-c)S_\mathrm{A}) \\ &= \mathrm{Var}\left(c\sum_i k_i S_i + (1-c)S_\mathrm{A}\right) \\ &= \left(c^2\sum_i k_i^2 + (1-c)^2\right)\sigma^2\end{aligned} \tag{5}$$

where σ^2 is the variance of the noise at each point, assumed for this to be constant throughout the eye. Now, we want to choose c to minimise this variability in the filtered value from Eq. (5), and so reduce the noise as much as possible. Mathematically, the minimum of a function occurs when its differential equals zero. So, differentiating

$$\begin{aligned}\frac{\mathrm{d}}{\mathrm{d}c}(\mathrm{Var}(S_\mathrm{A}^\mathrm{f})) &= \left(2c\sum_i k_i^2 - 2(1-c)\right)\sigma^2 = 0 \\ \left(\sum_i k_i^2 + 1\right)\hat{c} &= 1 \\ \hat{c} &= \left(\sum_i k_i^2 + 1\right)^{-1}\end{aligned} \tag{6}$$

So, we have a prescription from Eq. (6) for choosing c if the predicted values were completely accurate. However, this is clearly not the case; indeed, the predictions at some points will be closer to the raw values than elsewhere in the visual field. So, the correlations Corr_A between the predicted and raw values at each point A were found by calculating the predicted sensitivity at point A for each visual field in the database; so $\mathrm{Corr}_\mathrm{A} = \mathrm{Corr}(S_\mathrm{A}, \widehat{S}_\mathrm{A})$. This then provides a measure of the predictability of point A; the higher this correlation is, the more accurate the predicted sensitivity and so the more weight should be given to it in the filter. Now, $\hat{c}$ was found in Eq. (6) based on the assumption that the predicted values were 100% accurate; so in the final filter, the weighting given to the predicted sensitivity in the filter is given by $c = \hat{c} \times \mathrm{Corr}_\mathrm{A}$. So, having found the k_i for point A by multiple regressions (as described above), the final filtering algorithm for point A is

$$S_A^f = \frac{\mathrm{Corr}_A}{\sum_i k_i^2 + 1}\left(\sum_i k_i S_i\right) + \left(1 - \frac{\mathrm{Corr}_A}{\sum_i k_i^2 + 1}\right) S_A \qquad (7)$$

Obviously, the k_i differ according to which point in the visual field is being considered (point A); and so the filter is, in effect, a matrix containing the coefficients for filtering each point in the field, coefficients which vary from point to point.

2.2. Testing the filter

Visual fields are typically followed over a number of years to determine whether a suspected glaucomatous defect is progressing or not. It is proposed that this feature could provide an indication of the effectiveness of the filter. Indeed, the Gaussian filter has previously been shown to improve the consistency over time of visual fields (Crabb et al., 1997), which is one important aspect of reducing the noise.

Significantly, however, it has previously been reported that although the Gaussian filter may reduce noise, it also reduces the signal (Spry et al., 2002), i.e. methods which use filtering will be less successful at detecting localised defects than methods based on the raw data. It was decided to investigate this by looking at the effect of filtering on simulated visual field series, using pointwise linear regression (PLR) as the testing tool. The simulated data was generated by a previously developed "Virtual Eye", fully described elsewhere (Gardiner & Crabb, 2002a, 2002b). Briefly, this produces series of visual fields with known properties (baseline sensitivity values, length of series, frequency of testing, rates of loss) and adds noise by sampling randomly from a normal distribution, mean zero and with a standard deviation which increases (hence increasing the amount of noise) as the underlying sensitivity decreases, following a result from Henson, Chaundry, Artes, Faragher, and Ansons (2000). Using this "Virtual Eye" simulation, series of six fields (from annual testing over a period of 5 years) were simulated based on input noise-free visual fields; the simulation adds random noise to each of the six fields in the series. It was sought to make these noise-free series as simple as possible, to simplify and clarify the results obtained. So, each point in the field was assigned as one of

1. *Stable*: the sensitivity remains constant at 30 dB throughout the series, before noise is added.
2. *Defective*: the noise-free sensitivity is reduced by 2 dB per year, from 30 to 20 dB over the 5 years.
3. *Border*: the noise-free sensitivity is reduced by 1 dB per year, from 30 to 25 dB.

This process was first carried out on a 'stable' visual field; i.e. one where all 54 points in the visual field (including the two points coinciding with the blind spot) were *Stable*. Next, localised defects were chosen with reference to the map of the physiological optic nerve head (ONH) locations for each visual field test point produced by Garway-Heath, Poinoosawmy, Fitzke, and Hitchings (2000). The rationale for using this map is that localised defects are more likely to occur in clusters determined by the anatomical entry position of nerve fibre bundles into the optic disc. This rationale partly satisfies the need for determining localised defects separate from one based on perimetric data alone, avoiding the use of purely arbitrary and subjective defects. Using the map, a 'Central Point' was chosen, and its location in the ONH noted. This point and all other points located within ±5 degrees of the Central Point in the ONH were assigned as being *Defective* points with a glaucomatous loss of 2 dB per year. Further points between 6 and 10 degrees away from the Central Point (in terms of ONH location) were assigned as being *Border* points, with a glaucomatous loss of 1 dB per year. Points elsewhere in the eye were assumed to be *Stable*. Each of the 54 points in the standard visual field was considered in turn as the Central Point, with the exceptions of the two points forming the blind spot. Anderson's criteria (Anderson & Patella, 1999) define a clinically significant progressing localised defect as being a cluster of three or more points that have sensitivities occurring in fewer that 5% of the normal population, at least one of which must occur in less that 1% of the population, according to the pattern deviation probability plot. Hence, localised defects generated in this way which were found to consist of fewer than three adjacent points, and therefore not constituting an identifiable defect according to Anderson's criteria, were separated out and will be commented further upon later (this comprised six 'defects' consisting of a solitary point, and six 'defects' of just two points). Some examples of defects generated in the manner described are shown in Fig. 2.

Finally, the process was carried out on a field with a non-glaucomatous defect (as shown in Fig. 3), consisting of three Defective points with one Border point at each end. This was done in the hope that a filter designed to identify glaucomatous defects will not pick up defects which would not occur in glaucoma. Such a defect may be genuine, caused by for example a neurological disease; but since the purpose of this work is to more readily identify the existence and progression of glaucomatous defects, and it is not designed for use when other suspected conditions are being looked for, it is desirable that such non-glaucomatous defects be blurred out.

Each input series was simulated 5000 times. After each run, points were tested to see whether they would be flagged as progressing using a widely used PLR criterion. PLR is fully described elsewhere (Fitzke, Hitchings, Poinoosawmy, McNaught, & Crabb, 1996; Katz,

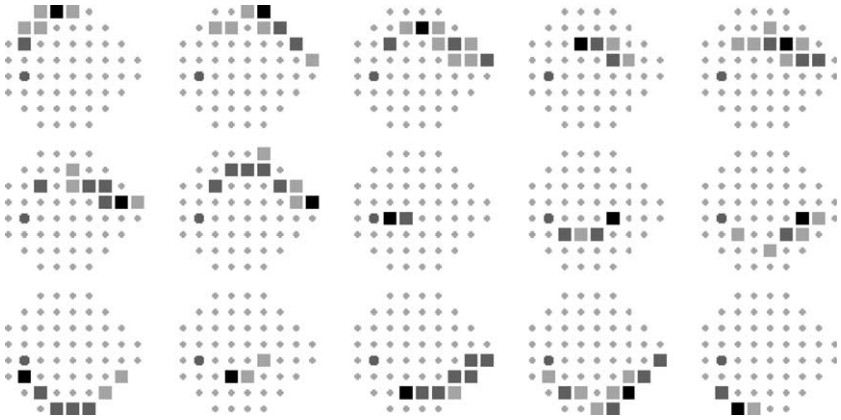

Fig. 2. The shapes of some of the 52 generated defects tested, superimposed onto a Humphrey 24-2 visual field. The black square in each case is the Central Point. Dark grey squares represent the Defective points (within 5 degrees of the Central Point in the ONH); light grey squares represent the Border points (between 6 and 10 degrees away from the Central Point in the ONH). The grey circle represents the location of the physiological blind spot.

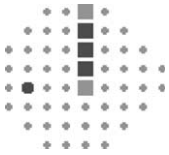

Fig. 3. The shape of the non-glaucomatous defect used, superimposed onto a Humphrey 24-2 visual field. As before, the grey circle represents the physiological blind spot.

Gilbert, Quigley, & Sommer, 1997; Smith, Katz, & Quigley, 1996; Wild, Hutchings, Hussey, Flanagan, & Trope, 1997) and is a form of change analysis whereby each individual field location is tested to find its pointwise rate of deterioration (slope) and a measure of statistical significance. The criteria for a progressive point used in these simulation experiments were a deterioration of at least 1 dB per year, statistically significant at the 1% level. This criteria has been used in published studies (Membrey, Bunce, Poinoosawmy, Fitzke, & Hitchings, 2001; Nouri-Mahdavi, Brigatti, Weitzman, & Caprioli, 1997; Viswanathan et al., 1999) and is examined in detail elsewhere (Gardiner & Crabb, 2002b). This analysis was repeated after filtering the noisy simulated series using each of the Gaussian and our new filter. So for each of the 5000 runs for each input series, the points were tested three times. In this way, the sample probabilities of the points being flagged as progressing based on each of the Raw, Gaussian and Filtered data were calculated. In the case of the input localised defects, the probabilities of the Central Point being (correctly) flagged as progressing in each case will hereafter be referred to as the three Detection Rates for that defect.

The computational derivation of the filter, the virtual eye simulation and additional statistical analyses were carried out using purpose written programs developed in S-PLUS for Windows (Insightful Corporation, Seattle, USA.).

3. Results

3.1. Shape of the filter

The filter conforms to the accepted physiological shape of the retinal nerve fibre layer. Fig. 4 shows the points that are used to filter a few Central Points (i.e. those points with a non-zero k_i when the relevant Central Point is 'point A' in the derivation above). If a point is connected to the Central Point by a line, it indicates that that point is a predictor for the Central Point; the thicker the line, the larger the effect it has on the prediction (i.e. the higher k_i is for that point). The remaining contribution to the filtered value comes from the Central Point itself. It is seen that predictors are not necessarily neighbours of the Central Point (as they would be if the Gaussian filter was being considered), but they follow the expected arcs. As seen in Fig. 1, this diagram for the Gaussian filter would simply connect each Central Point with all of its immediate neighbours.

Further, points on opposite sides of the horizontal meridian only turn out to be significant predictors on one occasion. This is very promising, since the derivation of the filter at no point took account of the relative

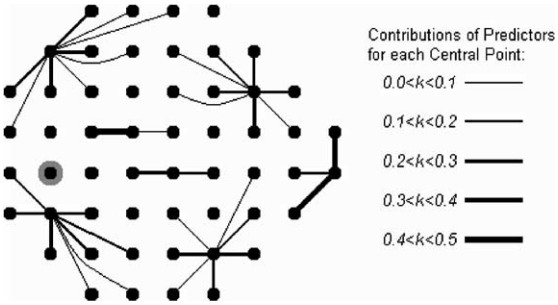

Fig. 4. An illustration of the shape of the filter. The grey area represents the blind spot.

positions of point in the visual field. The only location where a point does turn out to be a significant predictor of a point on the opposite side of the horizontal meridian is at the nasal step. This observation is interesting in itself, since nasal step defects are seen to cross the horizontal meridian in clinical practice. One possible explanation is the anatomical notion that some nerve fibres from upper and lower hemiretinas interdigitate at the temporal end of the horizontal raphe (Sakai, Kuniyoshi, Tsuzuki, Makoto, & Kawamura, 1987; Vrabec, 1966); alternatively, the phenomenon could be caused by local effects from the glaucomatous process (e.g. excitotoxicity) or a testing artefact. Also, the filter as derived above always assigns a sensitivity of zero to the point labelled in grey in Fig. 4, which corresponds to the blind spot (10–15 degrees temporal of the fovea, just below the horizontal meridian); again, this was not predetermined by the method of deriving the filtering algorithm.

3.2. Effect of the filter

Clearly, the noisier the initial (raw) visual field is, the more obvious to the naked eye will be the difference caused by filtering. Finding suitable visual fields which are noisy yet certainly have localised defects is near impossible. The effects of the filter are frequently subtler; although improvements undetectable when simply viewing greyscales of the data may have much larger effects over time when a computer analysis, such as PLR (Fitzke et al., 1996) or the Glaucoma Change Probability (Heijl et al., 1991), is used. However, there are cases when the benefits are clear for all to see. Fig. 5 shows a 24-2 greyscale from an eye, taken from a textbook example (Budenz, 1997), noted as having moderate to early glaucoma. There is a scotoma superior to the nasal horizontal meridian partially obscured by the noise present throughout the field. Filtering emphasises this defect, at the same time as removing most of the random noise elsewhere in the field. In contrast, the Gaussian filter almost entirely blurs out this defect. Note also that the new filter leaves the blind spot intact; the Gaussian filter may or may not do so, depending on the implementation.

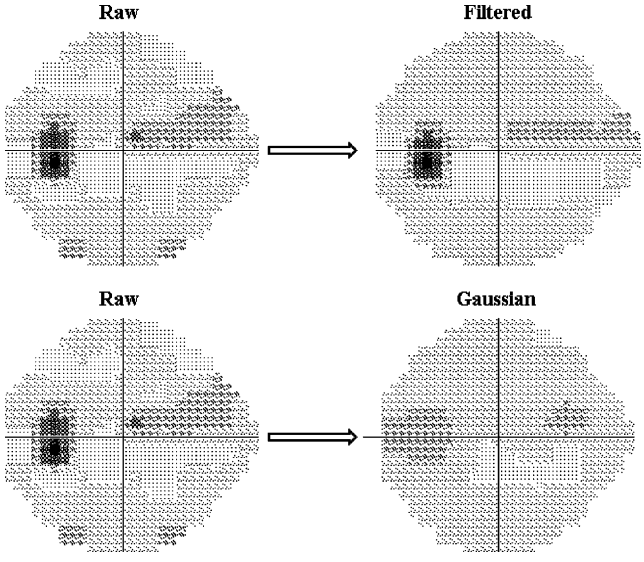

Fig. 5. The effect of the new filter on a visual field exhibiting a scotoma in the superior hemifield, compared with the effect of applying the Gaussian filter to the same data.

3.3. Virtual eye simulation

When the stable eye was tested (i.e. one where, before the addition of noise, all the points remain at a sensitivity of 30 dB throughout, as described above), the proportion of points still being flagged as progressing (all of which are therefore false positives) fell dramatically from 0.59% to 0.04% upon applying our new filter. This is further evidence that the filter is reducing the noise.

For each of the artificial localised defects based on the ONH structure (illustrated in Fig. 2), the percentage of the 5000 runs of the simulation which resulted in the Central Point satisfying the standard criteria for progression under PLR (i.e. a slope of at least −1 dB per year, statistically significant at the 1% level) was calculated. This percentage was found after the same 5000 noisy series had been filtered using the Gaussian filter (marked as 'Gaussian'), and using the new filter (marked as 'Filtered'), as well as before filtering (marked as 'Raw'). The results are shown in Fig. 6. The detection rates for the Central Points vary considerably after filtering, since they depend in part on the status of neighbouring points; without any filtering, the detection rates are consistently around 20% for the Central and Defective points (which are deteriorating at 2 dB per year) and around 8% for the Border points (which are deteriorating at 1 dB per year). It is seen that in almost all cases, the percentage of Central Points correctly identified as progressing increased significantly after filtering. Further, the new filter is performing much better than the Gaussian filter in this regard; it was common for defects to be blurred out by the Gaussian filter. The mean detection rate for the localised defects was 19.9% for the unfiltered, raw data; rising to 29.9% after application of the Gaussian filter, and 38.0% after using our new filter.

Of the 54 possible Central Points in the central visual field, 14 resulted in defects consisting of fewer than three adjacent points and so did not satisfy the criteria of Anderson and Patella (1999) (comprising the two points coinciding with the physiological blind spot, six solitary point 'defects', and six two point 'defects'). Because they did not produce realistic glaucomatous defects

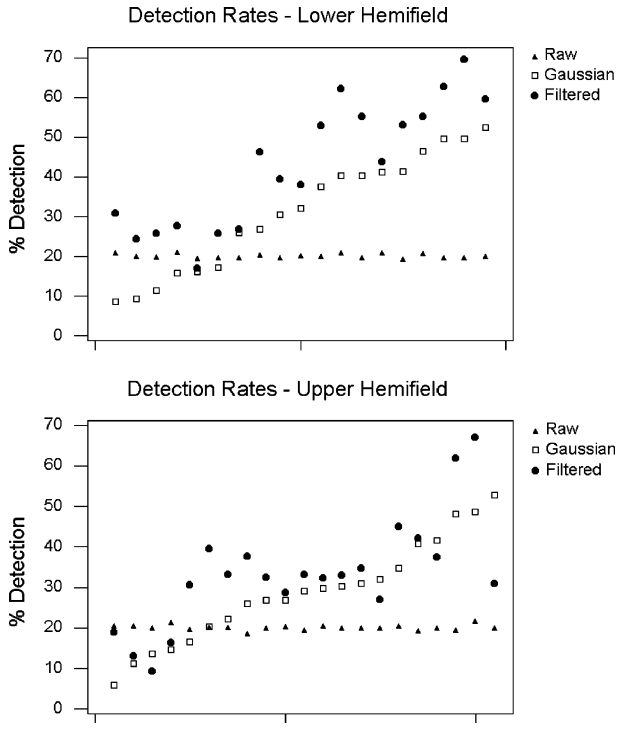

Fig. 6. Percentage of Central Points correctly flagged as progressing for each of the tested defects. Each column contains three symbols, representing the detection rates for the raw data, the data after application of the Gaussian filter, and the rate after application of our new filter; there is one column per point tested. The points have been split into the two hemifields. The points are in each case shown in order of increasing detection rate after application of the Gaussian filter (rather than in order of location), to make the figure clearer to understand.

(according to this definition), results from these 14 Central Points are not included in Fig. 6. However, this does not necessarily mean that these small defects were not picked up. Indeed, the two-point localised defect in the centre of the field next to the blind spot, illustrated by the central field in Fig. 2, resulted in the detection rate increasing from 19.9% to 37.1% after filtering. Certainly, as with any type of spatial filtering, if a defect consists of only one solitary point its detection rate will decrease. However, one deteriorating location may not constitute clinical glaucomatous progression.

Of more concern are the five Central Points for which the detection rate in Fig. 6 appears to be reduced by filtering. These five defects are those shown in Fig. 7. In each case, the apparent reduction in the detection rate caused by filtering is explained by the differences in shape between the defect being tested (generated from the ONH map) and the shape of the filter at that point which is shown in the bottom row of Fig. 7 (generated from visual field data). A large proportion of the filtered value for the Central Point is based on points not appearing in the defect; over 50% for defects A, D and E, and between 40% and 50% for defects B and C. These five isolated cases appear to behave in this way because of the method used for generating simulated defects, and are not necessarily reason to doubt the usefulness of the filter. Furthermore, in the first three cases, the overall detection rate taken over all the points which are deteriorating at 2 dB per year (the Central Point, represented by the black square, and the Defective points represented by dark grey squares), rather than just the Central Point, has actually improved. With defect A, the average detection rate has in fact increased from 19.9% to 29.1% after filtering (Gaussian: 22.3%); although the Central Point itself is being flagged as progressing less frequently, the rest of the defect is more likely to be picked up, and so the overall detection rate has still improved. Similarly for defect B, where the average has increased from 19.6% to 21.5% (Gaussian: 23.6%); and for defect C, where the average has increased from 20.1% to 31.5% (Gaussian: 26.9%).

The non-glaucomatous defect shown in Fig. 3 was tested in the same way. Averaged over the three Defective points, the filter reduced the percentage of runs of the simulation which resulted in points being flagged as progressing from 19.7% to 10.0%; in effect blurring out non-glaucomatous defects, as hoped. The Gaussian filter did not have this beneficial effect; in fact it increased the proportion flagged from 19.7% to 29.6%.

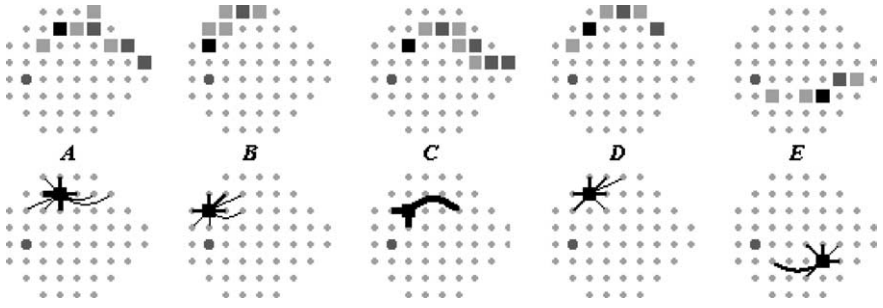

Fig. 7. The five generated localised defects whose detection rate appears to be reduced by filtering in Fig. 6, using the same symbols as in Fig. 2. The lower line shows the points involved in the filtering algorithm for that particular Central Point; the thicker the line, the more effect the point has on the filtered value for the Central Point.

4. Discussion

The principle of filtering real-world data is long established as a tool for reducing noise. Indeed, even in a standard measurement of the visual field with a Humphrey perimeter, double determinations of the sensitivity are carried out at certain points in the field; and while this is done principally to provide an estimate of the variability present in the readings, it also provides a basic form of filtering, as clinicians may base their judgment on the mean of these double determinations. The semi-Bayesian approach of using the prior expected sensitivity at a point to predict it before it is measured is also utilised in the SITA algorithm (Bengtsson et al., 1997). Spatial filtering, in the form of a Gaussian filter, has also been applied to visual field data with the benefit of reducing between test variability and improving the predictability of future visual field changes (Crabb et al., 1995, 1997; Fitzke et al., 1995). However, a recent study using a computer simulation of progressive glaucomatous visual field loss (Spry et al., 2002) concluded that Gaussian filtering does not offer a consistent benefit over the analysis of raw visual field data, and in some instances significantly inhibits the ability to detect small, gradual progressive field changes. In support of these findings, our testing of the Gaussian filter on our selection of localised defects also showed that, in some cases, it blurred out smaller progressive defects. With our new improved filtering algorithm, the detection of progressing points not only did not worsen, but it actually improved significantly, even in cases of small clusters of progressing points. The new filter also offers dramatic improvement in specificity when compared with unfiltered fields (reducing the false positive rate from 0.59% to 0.04%), vital for pointwise methods for detecting progression. Indeed, a seemingly small improvement in specificity may be more important than a larger improvement in sensitivity (Gardiner & Crabb, 2002b) (although here we are in the happy position of improving both!).

For any new method to become widespread in clinical use, it must be widely tested and demonstrated to provide a notable improvement on the current methodology. Opinions will naturally differ on what criteria are necessary for such a new method to be adopted. In this paper, a simulation method has been used to test the filter. Simulation, which is becoming an increasingly utilised tool in visual field problems (Gardiner & Crabb, 2002a, 2002b; Glass, Schaumberger, & Lachenmayr, 1995; Johnson, Chauhan, & Shapiro, 1992; Spenceley & Henson, 1996; Spry, Bates, Johnson, & Chauhan, 2000; Spry et al., 2002; Vesti, Spry, Chauhan, & Johnson, 2002), was used to test not only whether the noise was being reduced by filtering, but also whether true localised defects were being blurred out. The details of the simulation used, and its benefits and disadvantages, are discussed elsewhere (Gardiner & Crabb, 2002a, 2002b). With any simulation, the results should be viewed qualitatively rather than quantitatively, due to uncertainty over such issues as the amount of noise used etc. Nevertheless, these experiments have clearly shown that defects are emphasised by the new filter, whilst there are less false positives from stable points and non-glaucomatous defects.

The use of a map of the ONH for generating localised defects (Garway-Heath et al., 2000) has the notable advantage that it is not wholly based on perimetric results, thus making it suitable for independently selecting progressive defects. The rare instances of progressive defects where the new filter did not emphasise progression may tell us more about that lack of relationship between functional and structural change; or equally, may be a result of correlations forged as part of the testing strategy of the perimeter itself in establishing thresholds. Some correlation between points, whether contiguous or not, may well be the result of the testing strategy and not of the physiological connections. It was interesting to note that the perimetric data alone indicated correlation between the two nasal points either side of the horizontal meridian which is often noted clinically (Sakai et al., 1987; Vrabec, 1966). The effect of this is that the range of defects generated may not be entirely realistic or comprehensive. Further, it means that the detection rate being reduced by filtering in the cases of two of the tested defects (defects D and E in Fig. 7) need not be considered a problem with the filter; more, it may point to a difference between the structural and functional maps of the eye at those points. It is perfectly believable, and in fact to be expected, that there will be a few points in the eye where the results from this testing technique would not be perfect even if the filter were. This is a limitation of using this method for choosing realistic localised defects; yet this is preferable to choosing defects in a completely subjective manner based on common beliefs about visual fields, which would be biased towards the expected shapes.

Naturally, any further testing is to be welcomed. It would be desirable to also test whether or not localised defects are blurred out by filtering by looking at the real patient data. This is hampered by the lack of a definition in the literature of what constitutes an expected defect; progressing or otherwise (hence why our simulation uses shapes of the localised defects generated by looking at a physiological map of the ONH). One possibility which is currently being considered is to look at the predictive power of trend analysis methods, in the hope that this power would increase once the data had been filtered; however to do this would require a clean, independent database, and so it has not been carried out to date. Despite these inherent problems, and although the results of simulation should not be underestimated, they still need to be confirmed by clinical observations.

It should be emphasised that the filter described here is designed solely for suspected glaucoma patients. It is based on data from a glaucoma clinic, and so resembles the shapes of glaucomatous defects. This means that it is unsuitable for use when other conditions are suspected; neurological defects, for example, will be blurred out by the use of this filter, as demonstrated by the effect of the filter on the defect shown in Fig. 3. Of course, when the issue is whether the patient has glaucoma or not, or whether their glaucoma is progressing, it is entirely desirable that non-glaucomatous defects be blurred out.

Even without further testing, there is sufficient evidence presented here to say that the new filter shows clinical potential, especially since it requires no changing of visual field testing or extra patient test time. It is to be hoped that the filter technique described here could in the future become a widely accepted tool in glaucoma clinics.

Acknowledgements

The authors would like to thank David Garway-Heath and Ananth Viswanathan of the Glaucoma Unit, Moorfields Eye Hospital, London for advice during the preparation of this manuscript.

References

Anderson, D. R., & Patella, V. M. (1999). *Automated static perimetry* (2nd ed.). St. Louis, MO: Mosby, pp. 147–159.

Artes, P. H., Iwase, A., Ohno, Y., Kitazawa, Y., & Chauhan, B. C. (2002). Properties of perimetric threshold estimates from Full Threshold, SITA Standard, and SITA Fast strategies. *Investigative Ophthalmology and Visual Science., 43*, 2654–2659.

Bengtsson, B., Olsson, J., Heijl, A., & Rootzén, H. (1997). A new generation of algorithms for computerized threshold perimetry SITA. *Acta Ophthalmologica Scandinavica, 75*, 368–375.

Budenz, D. L. (1997). *Atlas of visual fields*. Philadelphia, PA: Lippincott-Raven, pp. 146–155.

Chauhan, B. C., & House, P. H. (1991). Intratest variability in conventional and high-pass resolution perimetry. *Ophthalmology, 98*, 79–83.

Chauhan, B. C., & Johnson, C. A. (1999). Test–retest variability of frequency-doubling perimetry and conventional perimetry in glaucoma patients and normal subjects. *Investigative Ophthalmology and Visual Science, 40*, 648–656.

Crabb, D. P., Edgar, D. F., Fitzke, F. W., McNaught, A. I., & Wynn, H. P. (1995). New approach to estimating the variability in visual field data using an image processing technique. *British Journal of Ophthalmology, 79*, 213–217.

Crabb, D. P., Fitzke, F. W., McNaught, A. I., Edgar, D. F., & Hitchings, R. A. (1997). Improving the prediction of visual field progression in glaucoma using spatial processing. *Ophthalmology, 104*, 517–524.

Fitzke, F. W., Crabb, D. P., McNaught, A. I., Edgar, D. F., & Hitchings, R. A. (1995). Image processing of computerised visual field data. *British Journal of Ophthalmology, 79*, 207–212.

Fitzke, F. W., Hitchings, R. A., Poinoosawmy, D. P., McNaught, A. I., & Crabb, D. P. (1996). Analysis of visual field progression in glaucoma. *British Journal of Ophthalmology, 80*, 40–48.

Flammer, J., Drance, S. M., & Zulauf, M. (1984). Differential light threshold: short- and long-term fluctuation in patients with glaucoma, normal controls, and patients with suspected glaucoma. *Archives of Ophthalmology, 102*, 704–706.

Gardiner, S. K., & Crabb, D. P. (2002a). Frequency of testing for detecting visual field progression. *British Journal of Ophthalmology, 86*, 560–564.

Gardiner, S. K., & Crabb, D. P. (2002b). Examination of different pointwise linear regression methods for determining visual field progression. *Investigative Ophthalmology and Visual Science, 43*, 1400–1407.

Garway-Heath, D. F., Poinoosawmy, D., Fitzke, F. W., & Hitchings, R. A. (2000). Mapping the visual field to the optic disc in normal tension glaucoma eyes. *Ophthalmology, 107*, 1809–1815.

Glass, E., Schaumberger, M., & Lachenmayr, B. J. (1995). Simulations for FASTPAC and the standard 4-2 dB full threshold strategy of the Humphrey field analyser. *Investigative Ophthalmology and Visual Science, 36*, 1847–1854.

Heijl, A., Lindgren, G., Lindgren, A., Olsson, J., Asman, P., Myers, S., & Patella, M. (1991). Extended empirical statistical package for evaluation of single and multiple fields in glaucoma: Statpac 2. In R. P. Mills & A. Heijl (Eds.), *Perimetry update 1990/1991* (pp. 303–315). Amsterdam: Kugler & Ghedini.

Heijl, A., Lindgren, G., & Olsson, J. (1989). Test retest variability in glaucomatous visual fields. *American Journal of Ophthalmology, 108*, 130–135.

Henson, D. B., Chaundry, S., Artes, P. H., Faragher, E. B., & Ansons, A. (2000). Response variability in the visual field: comparison of optic neuritis, glaucoma, ocular hypertension, and normal eyes. *Investigative Ophthalmology and Visual Science, 41*, 417–421.

Johnson, C. A., Chauhan, B. C., & Shapiro, L. R. (1992). Properties of staircase procedures for estimating thresholds in automated perimetry. *Investigative Ophthalmology and Visual Science, 33*, 2966–2974.

Katz, J., Gilbert, D., Quigley, H. A., & Sommer, A. (1997). Estimating progression of visual field loss in glaucoma. *Ophthalmology, 104*, 1017–1025.

Lachenmayr, B. J., & Vivell, P. M. O. (1993). *Perimetry and its clinical correlations*. Stuttgart: Georg Thieme Verlag.

Membrey, W. L., Bunce, C., Poinoosawmy, D. P., Fitzke, F. W., & Hitchings, R. A. (2001). Glaucoma surgery with or without adjunctive antiproliferatives in normal tension glaucoma: 2. Visual field progression. *British Journal of Ophthalmology, 85*, 696–701.

Nouri-Mahdavi, K., Brigatti, L., Weitzman, M., & Caprioli, J. (1997). Comparison of methods to detect visual field progression in glaucoma. *Ophthalmology, 104*, 1228–1236.

Sakai, T., Kuniyoshi, S., Tsuzuki, K., Makoto, U., & Kawamura, Y. (1987). Temporal raphe of the retinal nerve fiber layer revealed by medullated fibers. *Japanese Journal of Ophthalmology, 31*, 655–658.

Smith, S. D., Katz, J., & Quigley, H. A. (1996). Analysis of progressive change in automated visual fields in glaucoma. *Investigative Ophthalmology and Visual Science, 37*, 1419–1428.

Spenceley, S. E., & Henson, D. B. (1996). Visual field test simulation and error in threshold estimation. *British Journal of Ophthalmology, 80*, 304–308.

Spry, P. G. D., Bates, A. B., Johnson, C. A., & Chauhan, B. C. (2000). Simulation of longitudinal threshold visual field data. *Investigative Ophthalmology and Visual Science, 41*, 2192–2200.

Spry, P. G. D., & Johnson, C. A. (2002). Identification of progressive glaucomatous visual field loss. *Survey of Ophthalmology, 47*, 158–173.

Spry, P. G. D., Johnson, C. A., Bates, A. B., Turpin, A., & Chauhan, B. C. (2002). Spatial and temporal processing of threshold data for

detection of progressive glaucomatous visual field loss. *Archives of Ophthalmology, 120*, 173–180.

Vesti, E., Spry, P. G. D., Chauhan, B. C., & Johnson, C. A. (2002). Sensitivity differences between real-patient and computer-simulated visual fields. *Journal of Glaucoma, 11*, 35–45.

Viswanathan, A. C., McNaught, A. I., Poinoosawmy, D., Fontana, L., Crabb, D., Fitzke, F., & Hitchings, R. (1999). Severity and stability of glaucoma: patient perception compared with objective measurement. *Archives of Ophthalmology, 117*, 450–454.

Vrabec, F. (1966). The temporal raphe of the human retina. *American Journal of Ophthalmology, 62*, 926–938.

Wild, J. M., Hutchings, N., Hussey, M. K., Flanagan, J. G., & Trope, G. E. (1997). Pointwise univariate linear regression of perimetric sensitivity against follow-up time in glaucoma. *Ophthalmology, 104*, 808–815.

Wild, J. M., Pacey, I. E., O'Neill, E. C., & Cunliffe, I. A. (1999). The SITA perimetric threshold algorithms in glaucoma. *Investigative Ophthalmology and Visual Science, 40*, 1998–2009.

Wild, J. M., Searle, A. E. T., Dengler-Harles, M., & O'Neill, E. C. (1991). Long-term follow-up of baseline learning and fatigue effects in the automated perimetry of glaucoma and ocular hypertensive patients. *Acta Ophthalmologica Scandinavica, 69*, 210–216.